ELECTRONIC TRANSPORT PROPERTIES (LOW TEMPERATURE HALL EFFECT MEASUREMENT) OF WSe_2 SINGLE CRYSTAL

C. A. Patel[1], K. D. Patel[2] and Kaushik R. Patel[3*]

Pilvai Science College, Pilvai (Gujarat)

[2] Department of Physics, Sardar Patel University, Vallabh Vidyanagar (Gujarat)

[3] Biogas Research and Microbiology Department, Gujarat Vidyapith, Sadra

****Author for Correspondence Email: krpatel@gujaratvidyapith.org***

Abstract

WSe_2 crystals grown by Direct Vapour Transport (DVT) technique. The structural properties of as grown crystals have been measured by X-ray diffraction analysis. The temperature dependence Hall coefficient study revealed that the grown crystal shows mixed conduction behavior in the temperature region 300K to 10K. The variation of mobility with temperature, also show that the WSe_2 possesses a mixed scattering mechanism. The Hall scattering factor calculated from the temperature dependent Hall coefficient and carrier density. Detailed analysis of temperature dependent Hall effect data thus yields information concerning the electronic transport properties of tungsten diselenide semiconducting layered materials.

1. INTRODUCTION

Electrical properties of materials play an important role in determining the behavior of solid state devices and thereby their potential for such applications. Investigations regarding the electrical behavior of Tungsten diselenide single crystals grown by direct vapor transport technique have been reported to be highly depended on growth conditions [1]. For its application in the device fabrication as a substrate material it must be thoroughly characterized for electrical transport properties. Hall Effect measurement is a unique tool to provide basic material parameters needed to find the suitability of its application. In the present investigation the Hall effect measurements were made using Lake Shore Hall measurement system 7504 over a range of temperature (300-10K) with the help of Lakeshore temperature controller (Model 340) and a Closed Cycle Refrigerator (CCR 75014) under a magnetic field of ±2.5kG to ±5kG.

The theoretical foundation of Hall measurement evaluation for irregularly shaped samples is based on conformal mapping developed by van der Pauw [2, 3]. He showed how the resistivity, carrier concentration and mobility of a flat sample of arbitrary shape can be determined without knowing the current pattern, if the following conditions such as:

(i) the contacts are sufficiently small,

(ii) the contacts are at the circumference of the sample

(iii) the sample is uniformly thick and

(iv) the sample contains no isolated holes are met.

Van der Pauw suggested different geometries such as circular, square, rectangular and cross. The cross structure generally used for films and other for bulk crystals.

According to the investigations made by Daniel W. Koon [4-7] for different geometries, the preferred geometry is square rather than circle to reduce the effect of contact lead placement errors in measurement of transport parameters such as resistivity and Hall coefficient. The square is the most convenient sample shape to fabricate, and by using a square shape sample reduce the effect of errors in the van der Pauw method arising from either the size or displacement of contact leads from the edge of the sample can be reduced. The lead placement in the square sample must be near the corners in order to minimize errors.

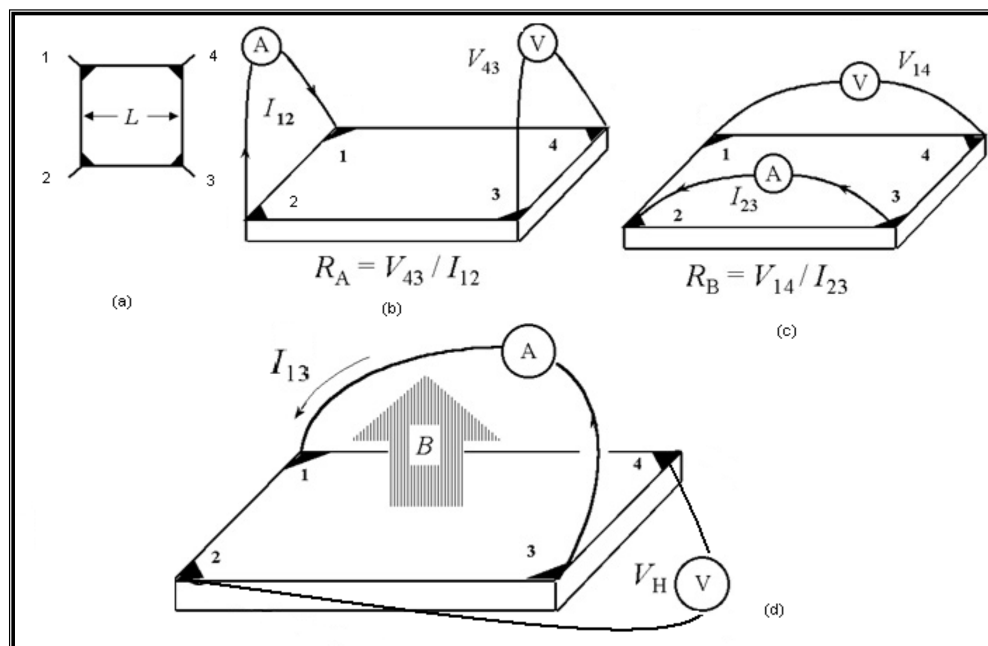

Figure 1: (**a**) Sample geometry for van der Pauw resistivity and Hall effect measurements. (**b**) and (**c**) Schematic of a van der Pauw configuration used in the determination of the two characteristic resistances R_A and R_B. (**d**) Schematic of a van der Pauw configuration used in the determination of the Hall voltage V_H

It is easy to show that for four contacts on the boundary of a semi-infinite plane sheet the resistances $R_{12,34}, R_{23,41}$ satisfy the relationship:

$$\exp\left(-\frac{\pi R_{12,34} t}{\rho}\right) + \exp\left(-\frac{\pi R_{23,41} t}{\rho}\right) = 1 \quad (1)$$

By knowing t, $R_{12,34}, R_{23,41}$ the above equation can be solved for the resistivity of the material, [8, 9],

$$\rho = \frac{\pi t}{\ln(2)} \frac{(R_{12,34} + R_{23,41})F}{2} \tag{2}$$

where, $$R_{12,34} = \frac{V_{34}}{I_{12}} \tag{3}$$

The current I enters the sample through contact 1 and leaves through contact 2 and $V_{34} = V_4 - V_3$ is the voltage between contacts 4 and 3. $R_{34, 41}$ is similarly defined. The quantity 'F' is a transcendental function of the ratio,

$$R_r = \frac{V_{43} I_{23}}{I_{12} V_{14}} = \frac{R_{12,34}}{R_{23,41}} \tag{4}$$

or $$R_r = \frac{I_{12} V_{14}}{V_{43} I_{23}} = \frac{R_{23,14}}{R_{12,43}} \tag{5}$$

Whichever is greater, and F is found by solving the equation,

$$\frac{R_r - 1}{R_r + 1} = \frac{F}{\ln(2)} ar\cosh\left\{\frac{\exp\left[\frac{\ln(2)}{F}\right]}{2}\right\} \tag{6}$$

F=1, when R_r=1, which occurs with symmetrical samples like circles or squares, when the contacts are equally spaced and symmetrical.

For each measurement point in a Hall experiment, up to 32 individual resistance measurements are required to be made for both A and B type of geometries. Here geometry A corresponds to $R_{12,43}$ and $R_{23,14}$ and geometry B corresponds to $R_{41,32}$ and $R_{34,21}$. Each van der Pauw resistivity requires 8 measurements (terminal interchange and current reversal for both figure 1(b and c) and the Hall resistance requires 4 measurements (terminal interchange and current reversal for figure 1 d).

The sequence of the measurements is as follows.

(i) Zero field resistance measurements (8 measurements).

(ii) Hall resistance measurements for +ve magnetic field, +B(4 measurements).

(iii) Resistivity measurements for +ve magnetic field, +B(8 measurements).

(iv) Hall resistance for –ve magnetic field, –B (4 measurements).

(v) Resistivity measurements for –ve magnetic field, -B(8 measurements).

In the present investigation the experiment has been conducted with a maximum magnetic field of ±5KG and for a lower temperature range of 300-10K.

By knowing the thickness 't' of the sample and measurement of voltage and current with polarity reversal across the contacts, the resistivities for geometries A and B can be calculated from the following equations [7 & 8).

$$\rho_A = \frac{\pi f_A t[m,cm]}{\ln(2)}\left(\frac{V_{12,43}^{+} - V_{12,43}^{-} + V_{23,14}^{+} - V_{23,14}^{-}}{I_{12}^{+} - I_{12}^{-} + I_{23}^{+} - I_{23}^{-}}\right)[\Omega.m, \Omega.cm] \tag{7}$$

and

$$\rho_B = \frac{\pi f_B t[m,cm]}{\ln(2)}\left(\frac{V_{34,21}^{+} - V_{34,21}^{-} + V_{41,23}^{+} - V_{41,23}^{-}}{I_{34}^{+} - I_{34}^{-} + I_{41}^{+} - I_{41}^{-}}\right)[\Omega.m, \Omega.cm] \tag{8}$$

here $V_{12,43}^{+}$ means voltage measured between contact 4 and 3 when positive forced current is allowed to pass between contact 1 and 2. Similarly I_{12}^{+} denotes +ve forward current measured between contacts 1 and 2. The geometrical factors f_A and f_B are functions of Q_A and Q_B, respectively, given by,

$$Q_A = \left(\frac{R_{12,43}^{+} - R_{12,43}^{-}}{R_{23,14}^{+} - R_{23,14}^{-}}\right) = \left(\frac{V_{12,43}^{+} - V_{12,43}^{-}}{I_{12}^{+} - I_{12}^{-}}\right)\left(\frac{I_{23}^{+} - I_{23}^{-}}{V_{23,14}^{+} - V_{23,14}^{-}}\right) \tag{9}$$

$$Q_B = \left(\frac{R_{34,21}^{+} - R_{34,21}^{-}}{R_{41,23}^{+} - R_{41,23}^{-}}\right) = \left(\frac{V_{34,21}^{+} - V_{34,21}^{-}}{I_{34}^{+} - I_{34}^{-}}\right)\left(\frac{I_{41}^{+} - I_{41}^{-}}{V_{41,23}^{+} - V_{41,23}^{-}}\right) \tag{10}$$

The relationship between f and Q is expressed by the transcendental equation,

$$\frac{Q-1}{Q+1} = \frac{f}{\ln 2}\cosh^{-1}\left(\frac{1}{2}\exp\left[\frac{\ln 2}{f}\right]\right) \tag{11}$$

The two resistivities must agree to within $\pm 10\%$. If they do not, then the sample is too inhomogeneous or anisotropic or has some other problem. If they agree, the average resistivity is given by,

$$\rho_{av} = \frac{\rho_A + \rho_B}{2}[\Omega.m, \Omega.cm] \tag{12}$$

Similarly with the help of same measurements of voltage and current along with the magnetic field reversal the two Hall coefficients are calculated by the following equations.

$$R_{HC} = \frac{t(m)}{B(T)}\left[\frac{V_{31,42}^{+}(+B) - V_{31,42}^{-}(+B) + V_{31,42}^{-}(-B) - V_{31,42}^{+}(-B)}{I_{31}^{+}(+B) - I_{31}^{-}(+B) + I_{31}^{-}(-B) - I_{31}^{+}(-B)}\right]\left[m^3.C^{-1}\right] \tag{13}$$

and

$$R_{HD} = \frac{t(m)}{B(T)}\left[\frac{V_{42,13}^{+}(+B) - V_{42,13}^{-}(+B) + V_{42,13}^{-}(-B) - V_{42,13}^{+}(-B)}{I_{42}^{+}(+B) - I_{42}^{-}(+B) + I_{42}^{-}(-B) - I_{42}^{+}(-B)}\right]\left[m^{3}.C^{-1}\right] \quad (14)$$

where R_{HC} and R_{HD} are the Hall coefficients for configuration shown in figure 1(d) and its terminal interchange respectively. These two should also agree to within ±10%. If they do not agree, it indicates that the sample is too inhomogeneous or anisotropic or has some other problem. If they agree, then the average Hall coefficient can be calculated by,

$$R_{Hav} = \frac{R_{HC} + R_{HD}}{2}\left[m^{3}.C^{-1}\right] \quad (15)$$

From the average value of resistivity and Hall coefficient the Hall mobility can be calculated by,

$$\mu_{H} = \frac{|R_{HAv}|}{\rho_{Av}}\left[m^{2}.V^{-1}.S^{-1}\right] \quad (16)$$

where ρ_{Av} is the zero field resistivity.

2. EXPERIMENTAL

Crystals of WSe_2 were grown by direct vapour transport (DVT) method [10, 11, 12]. The microstructural examination of the surfaces of the as grown crystals as well as the metal deposited surfaces was accomplished with the help of Axiotech 100 reflected light microscope, by Carl Zeiss Jena, Germany. Crystals with flat shining surfaces were chosen with the help of microscope. These crystals were then washed in acetone to remove contaminations and to make the surface clean. It is kept in the oven for a couple of minutes at 60^{0}C to dry out the crystals completely.

In the present study the ohmic contacts on crystals along the basal plane were prepared. Here contacts were made from conductive Ag paste to fix up low strain thin Ag alloy wires (13,14) onto the basal plane of the crystal. The contacts were then annealed at 100^{0}C for 12 hours.

The crystals with contacts developed using methods mentioned above were fixed on a mica piece and then soldered on a sample holder PCB for the verification of ohmic nature of different pairs of contacts for all the samples. Further for studying the low temperature stability the crystals were mounted on the sample mount stage inside the Closed Cycle Refrigerator (CCR 75014) and contacts were soldered for external connections.

2.1 HALL EFFECT MEASUREMENT SYSTEM

The Lake Shore 7504 Series Hall Effect/Electronic Transport Measurement System is designed to measure electronic transport properties of electrically conductive materials. The system consists of advanced, integrated hardware and software. 7504 Series systems are easy to operate using the Lake Shore Hall Measurement System Software. The Hall System Software controls system instrumentation during an experiment and determines sample resistance, resistivity, Hall coefficient, Hall mobility and carrier concentration. The software can control magnetic field during measurements. Variation in temperature is made possible with the help of Lakeshore temperature controller (340) coupled with the Closed Cycle Refrigerator (CCR 75014).

2.1.1 General Hall Effect Measurement System Features

Following are the general features of any Hall measurement system.

(a) Measures Hall voltage, resistance, magnetoresistance, and current-voltage characteristics with one system

(b) Calculates resistivity, Hall coefficient, carrier concentration and mobility

(c) Allows contact characterization by measuring current-voltage (I-V) curves in most configurations.

(d) Measurement configurations capable of measuring samples with resistances ranging from mΩ to hundreds of GΩ.

(e) Varies magnetic field to determine the effects on materials.

(f) Reduces measurement time with a fully integrated, automated computer data collection system which makes measurements and calculates results.

(g) Displays real-time feedback of processed measurement data in both graphical and/or tabular format as the experiment is taking place.

(h) Controls, monitors, and changes instrument settings throughout the experiment using Hall System Software. The software includes individual instrument drivers for complete on-screen, virtual front panel control and operation of all instrumentation.

(i) Allows users to write custom programs in Visual BASIC or other languages to access the Hall System Software using the Object Linking and Embedding (OLE) interface.

(j) Produces more accurate, repeatable measurements by actively monitoring, controlling, and stabilizing magnetic flux density (field). It also produces excellent field stability with water cooled magnet coils, feedback control, high quality sensors, and advanced electronics.

The Lake Shore 7504Series Hall Effect/Electronic Transport Measurement System consists of an electromagnet which can produce a magnetic field of maximum 10kG with 4 inch

air gap between the two pole pieces. The necessary current is being supplied by the magnetic power supply (LS 689) with current and voltage limits of 0 to ±72 A and 0 to ±32 V respectively. The Model 450 is an extremely accurate full-featured gaussmeter that covers a wide range of magnetic fields and applications. The instrument provides easy-to-use front panel programming and a vacuum fluorescent alphanumeric display. This alphanumeric format allows for message-based front panel operation. Most operations can be performed and monitored through the front panel keypad and message display. The Model 450 measures fields in either gauss (G) or tesla (T). Set magnetic field ranges manually or with auto ranging. The gaussmeter measures both DC and AC magnetic field values. In DC operation, the display shows the DC field at the probe with the sign (orientation) followed by the appropriate field units. In AC operation, the display shows a Peak or RMS value for the field at the probe.

The low temperature experiment is made possible with the help of Lakeshore temperature controller (Model 340), which balances the cooling power provided by a Closed Cycle Refrigerator (CCR 75014) against two heater circuits. The block diagram of close cycle refrigerator based cryostat is shown in figure 2 and figure 3 shows a schematic of the central and measurement system used for I-V-T and low temperature Hall-effect measurements. Lake Shore Model 340 temperature controller is designed to work as an integral part of a cryogenic temperature control system. The Model 340 has many specialized features that uniquely qualify it for this difficult job. These features are built on a fundamentally sound design that can be used in many applications requiring stable and accurate control from cryogenic temperatures, to room temperature and above. The goal of a temperature control system is to balance the effect of heating and cooling to provide a stable temperature in an area of interest. In order to control temperature, one needs the following elements:

1. A heating source.
2. A cooling source.
3. A means to measure temperature.
4. A means to compare the measured temperature to a desired temperature (called the set point).
5. A means to make any necessary changes to heating, cooling, or both.

The first control loop consists of a temperature sensor and heater attached to the cold end of the refrigerator. The sample is located near the bottom of the copper sample well. It is separated from the sample well by helium exchange gas, and is at a significant distance from the refrigerator cold end. A temperature sensor mounted directly to the sample provides a much more accurate measure of the actual sample temperature. The heater for the second control loop

is located on the bottom of the sample well. The temperature sensor on the sample insert is used to control the second loop heater.

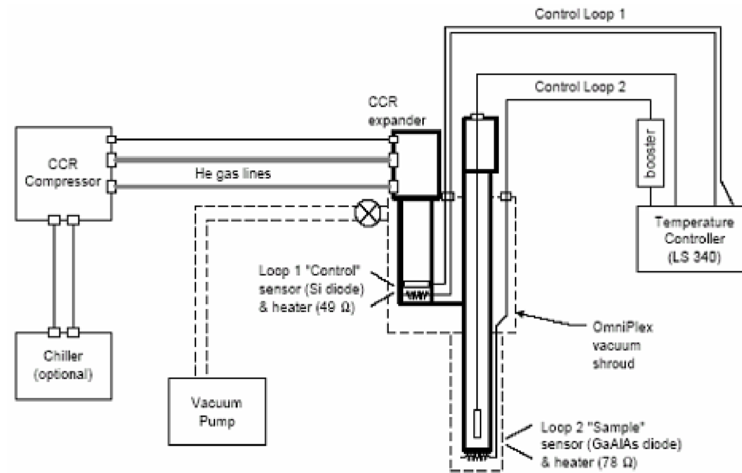

Figure 2: Block diagram of closed cycle refrigerator based cryostat used for I-V-T and low temperature Hall measurement.

Figure 3 Lakeshore-7504 complete Hall effect measurement system.

6.3 Results and Discussion

The experiment of low temperature Hall effect measurements have been conducted for number of samples prepared for Ohmic contacts as discussed above.

As an initial step of Hall Effect measurement, the ohmic nature of the electrical contacts made on the samples, the I-V characteristics have been verified shown in figure 4, before extracting the Hall parameters. In order to ensure the linear nature of the prepared electrical contacts, the contacts have been annealed.

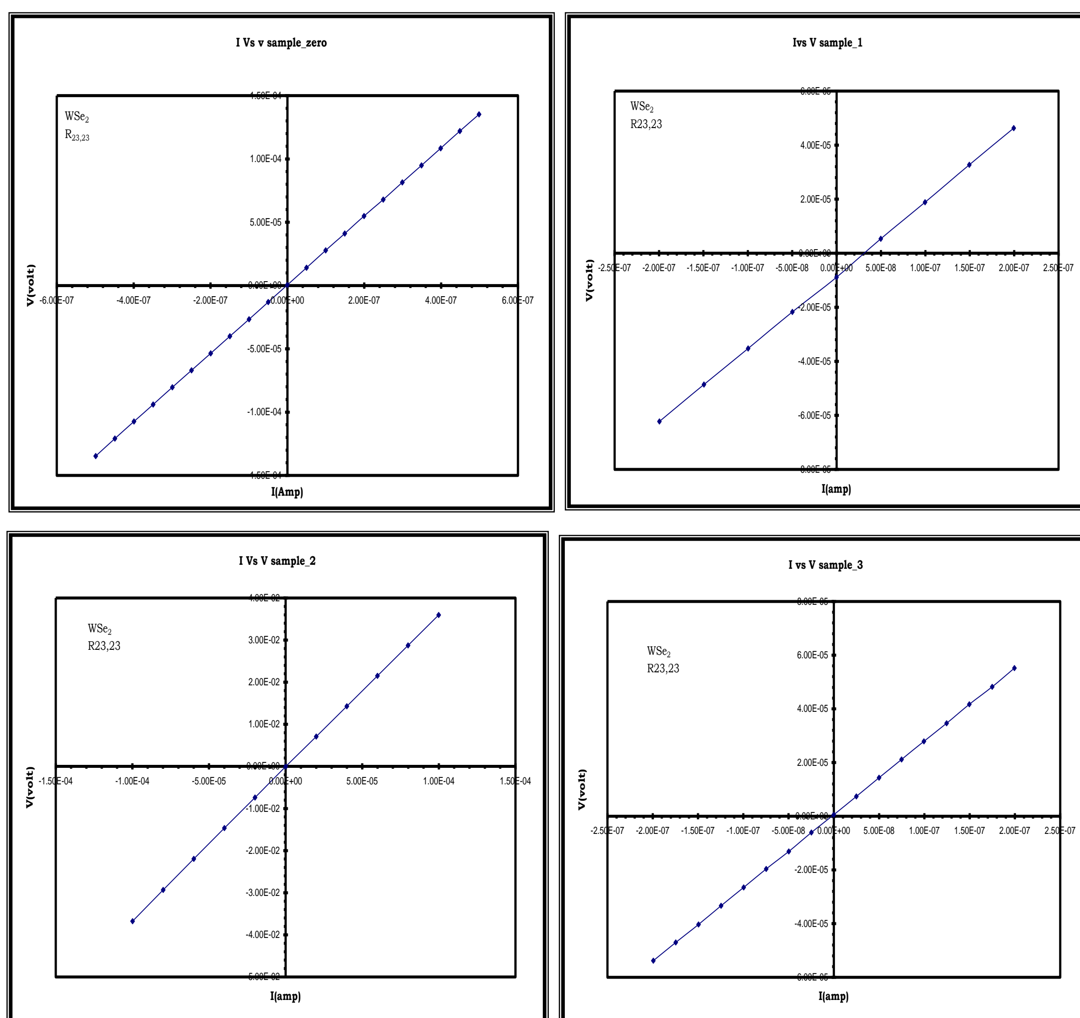

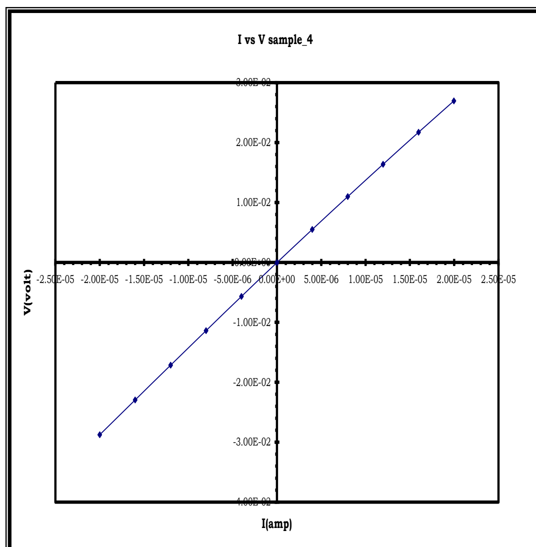
I vs V sample_4
V(volt)
I(amp)

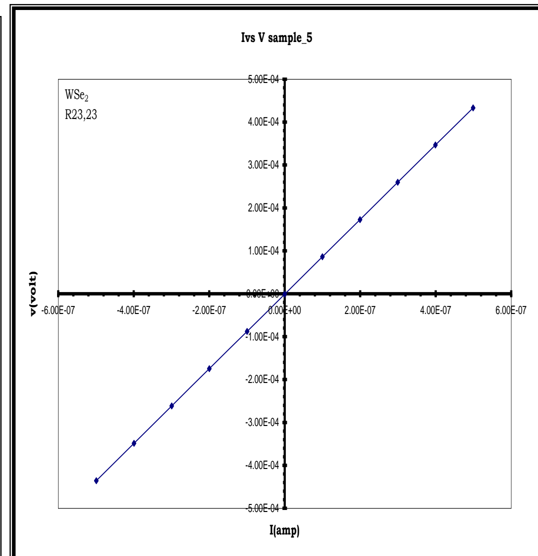
Ivs V sample_5
WSe_2
R23,23
v(volt)
I(amp)

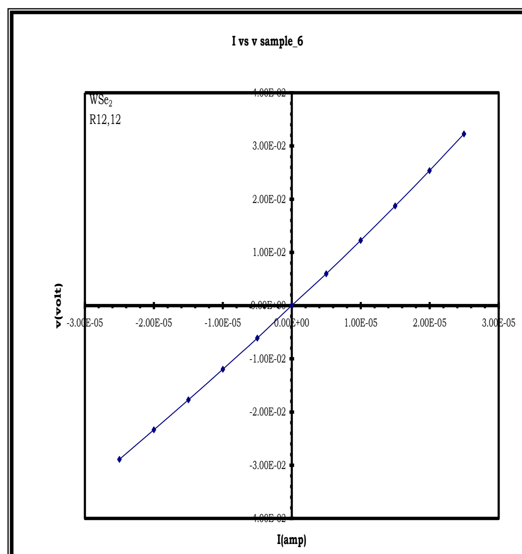
I vs v sample_6
WSe_2
R12,12
v(volt)
I(amp)

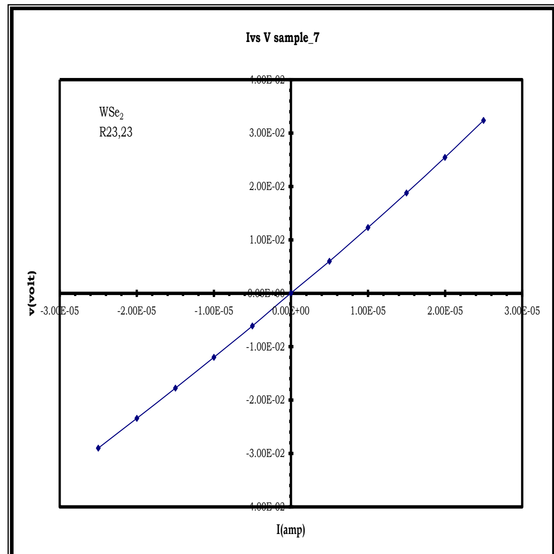
Ivs V sample_7
WSe_2
R23,23
v(volt)
I(amp)

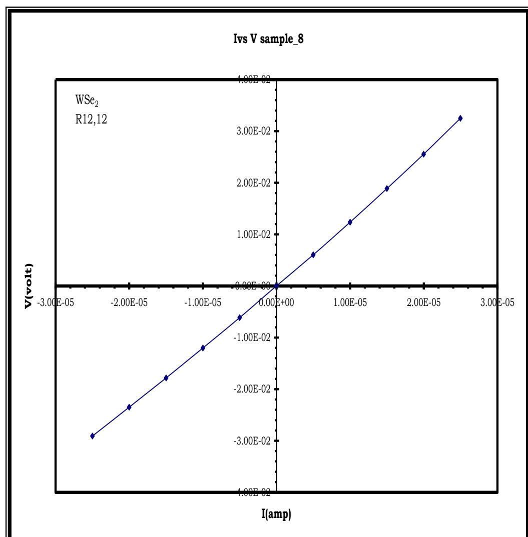
Ivs V sample_8
WSe_2
R12,12
v(volt)
I(amp)

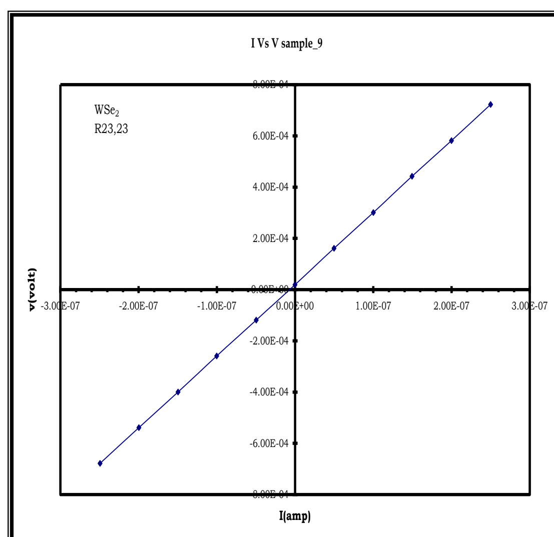
I Vs V sample_9
WSe_2
R23,23
v(volt)
I(amp)

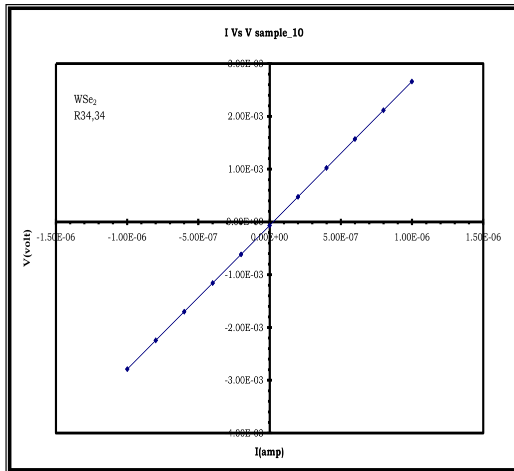
I Vs V sample_10
WSe2
R34,34
V(volt)
I(amp)

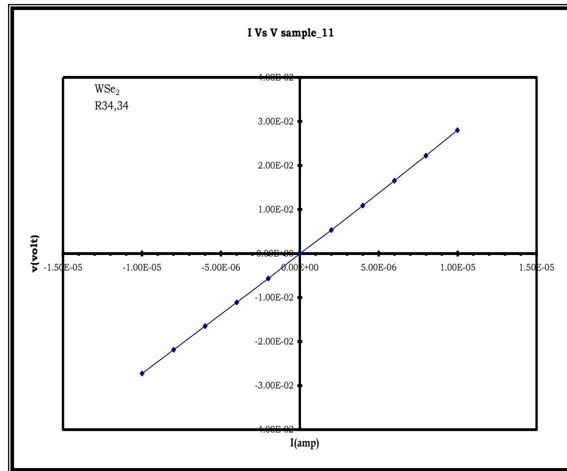
I Vs V sample_11
WSe2
R34,34
v(volt)
I(amp)

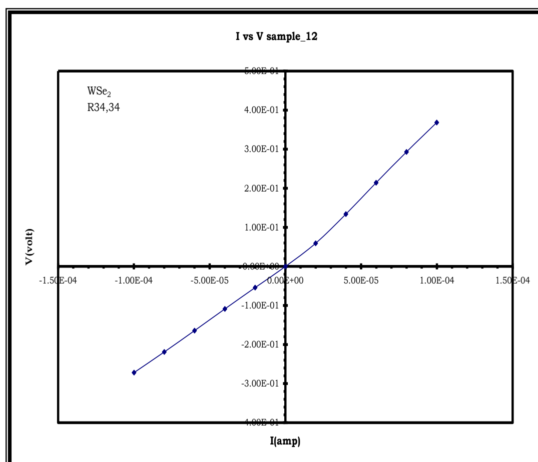
I vs V sample_12
WSe2
R34,34
V(volt)
I(amp)

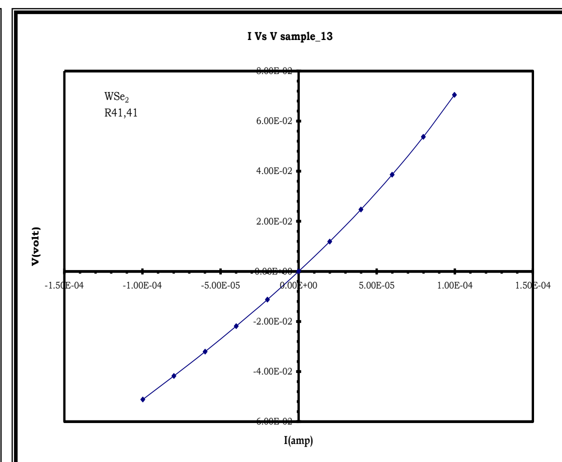
I Vs V sample_13
WSe2
R41,41
V(volt)
I(amp)

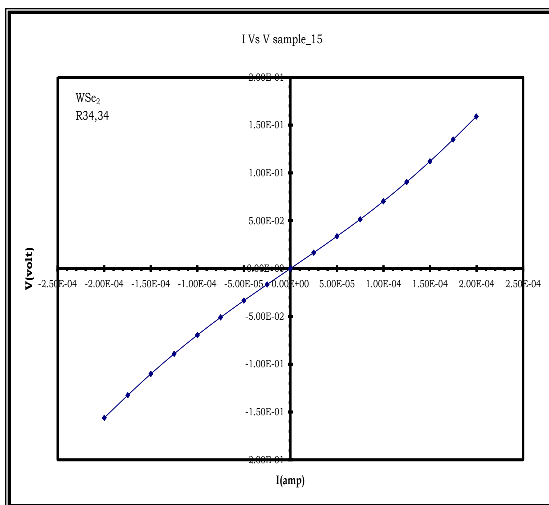
I Vs V sample_15
WSe2
R34,34
V(volt)
I(amp)

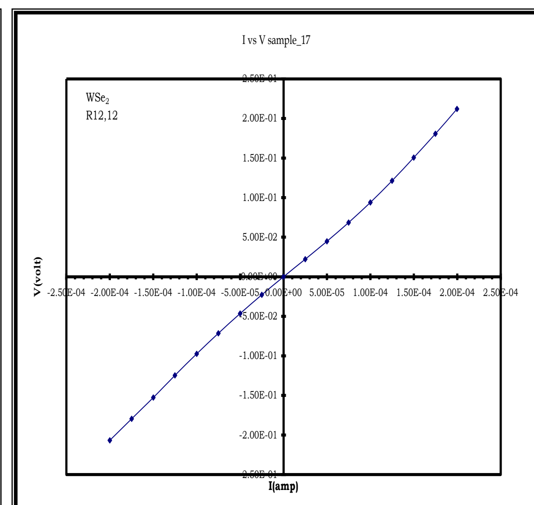
I vs V sample_17
WSe2
R12,12
V(volt)
I(amp)

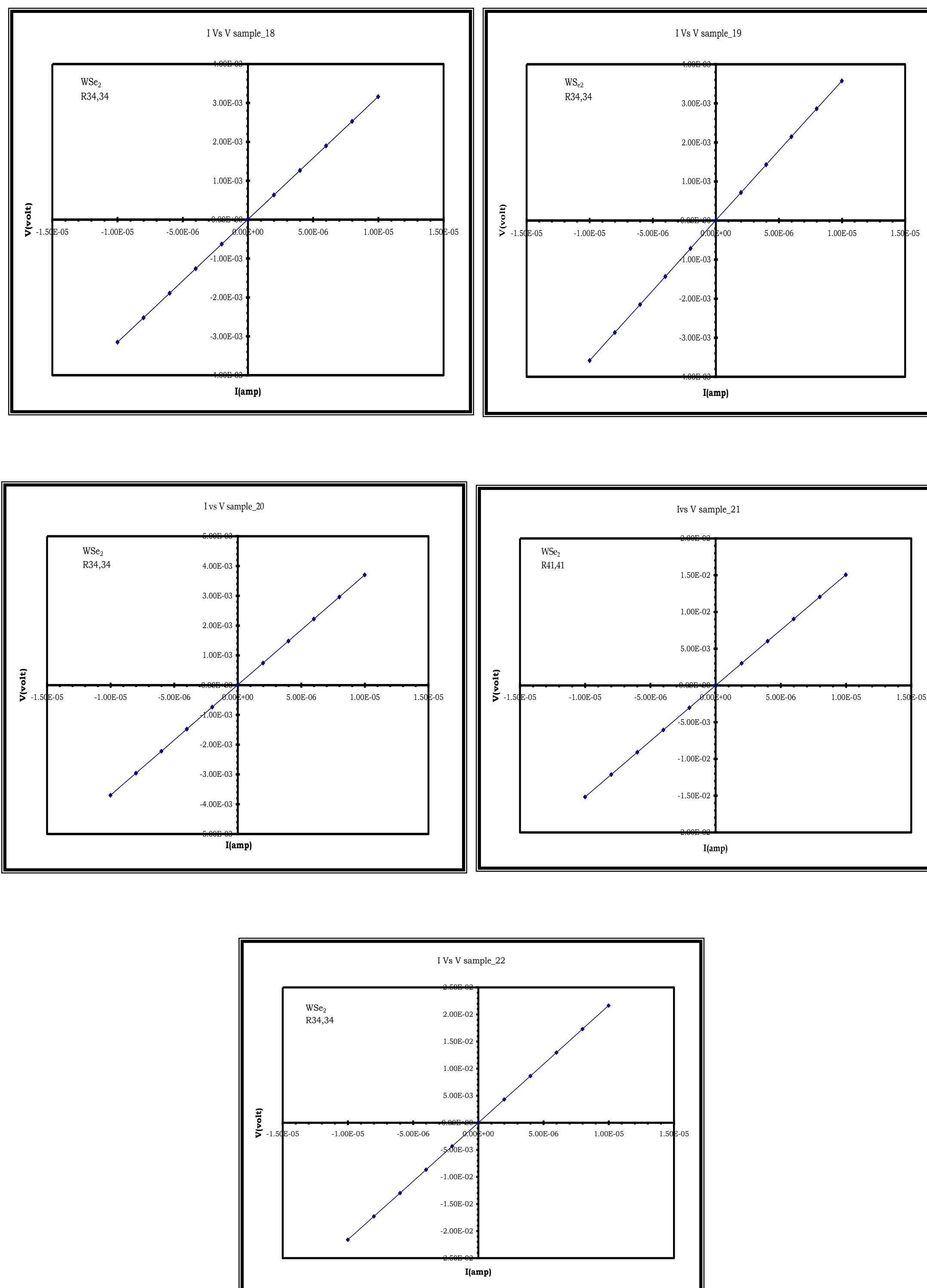

Figure 4: I-V plot for different samples (zero to Twenty two) to ensure the ohmic nature of WSe_2 single crystals

After the confirmation of the ohmic nature, experiment has been conducted for Hall parameters. An over view of the results thus obtained by these measurements, for different samples and different magnetic field at room temperature are tabulated in the Table 1.

Table 1: Room temperature Hall parameters of WSe_2 single crystal of various samples (1 to 22) for different magnetic field.

Sample no.	Factor A	Factor B	Resistivity (Ω.cm)	Carrier Density (cm^{-3})	Hall coefficient (cm^3/C)	Mobility (cm^2/Vs)	Magnetic Field in K.Gauss
1.	0.84	0.91	0.034	$3.03x10^{17}$	20.56	775.7	2.5 KG
2.	0.82	0.82	0.892	$3.54x10^{16}$	197.80	176.3	5 KG
3.	0.85	0.84	1.23	$2.35x10^{16}$	265.5	215.1	3 KG
4.	0.38	0.38	0.405	$3.78x10^{17}$	16.49	40.72	4 KG
5.	0.98	0.99	0.074	$8.54x10^{18}$	3.91	55.81	2.5 KG
6.	0.99	0.98	1.67	$1.40x10^{16}$	445.3	271.3	5 KG
7.	0.99	0.98	1.67	$1.37x10^{16}$	454.5	273.4	5 KG
8.	0.99	0.98	1.67	$1.35x10^{16}$	460	276	5 KG
9.	0.94	0.88	0.110	$6.41x10^{16}$	973.1	6517	2.5 KG
10.	0.99	0.99	0.271	$4.94x10^{16}$	126.3	441.4	3 KG
11.	0.88	0.97	0.2.6	3.24×10^{16}	192.1	866.9	3 KG
12.	0.98	0.98	0.227	4.21×10^{16}	54.45	239.6	3 KG
13.	0.98	0.98	0.572	7.33×10^{14}	85.08	148.7	5 KG
14.	1.00	1.00	1.057	3.17×10^{18}	1.96	1.86	3 KG
15.	0.74	0.74	0.471	6.35×10^{16}	98.23	208.3	3 KG
16.	1.00	1.00	1.059	3.24×10^{18}	1.93	1.82	3 KG
17.	0.91	0.90	0.603	5.37×10^{16}	116.1	192.4	3 KG
18.	0.27	0.28	0.205	1.48×10^{17}	42.16	211.1	3 KG
19.	0.27	0.28	0.203	1.44×10^{17}	43.3	214.6	4 KG
20.	0.26	0.27	0.200	2.28×10^{17}	27.3	135.3	4 KG
21.	0.97	0.97	2.87	4.55×10^{16}	137.2	48.43	4 KG
22.	0.98	0.97	2.80	1.03×10^{18}	6.049	2.14	4 KG

The value of van der pauw factor (VdPF) for geometry A ($R_{12, 43}$; $R_{23, 14}$) and B ($R_{34, 21;}$ $R_{41, 32}$) have been found to be in the range 0.26 to 1.00 and 0.27 to 1.00 respectively. It has been observed that among these samples many samples have good VdPF that means they predict a good ohmic behavior. Since few samples van der Pauw factors are not in the reliable range so the experiment has not been further extended to low temperatures for it. The low temperature

experiments were carried out for three samples for different temperature range and magnetic field to measure Hall parameters shown in Table 2 to 4

Table 2: Measured Hall parameters of WSe_2 single crystal (**sample:17**) in the temperature range **300K-75K** for **3KG** magnetic field

Temp. T(K)	Factor A	Factor B	Resistivity ρ(Ω.cm)	Carrier Density n(cm^{-3})	Hall coefficient R_H(cm^3/C)	Mobility μ (cm^2/Vs)
300	0.91	0.90	0.603	5.38×10^{16}	116.1	192.4
277	0.90	0.90	0.605	4.97×10^{16}	125.7	207.8
251	0.89	0.89	0.632	3.82×10^{16}	163.6	257.5
225	0.90	0.89	0.695	2.93×10^{16}	213.2	307.3
200	0.88	0.88	0.822	2.03×10^{16}	306.9	373.7
175	0.88	0.88	1.088	1.27×10^{16}	490	450.9
151	0.87	0.87	1.691	0.62×10^{16}	1003	595.7
125	0.87	0.86	3.621	0.25×10^{16}	2531	696.7
101	0.85	0.84	13.856	0.05×10^{16}	11150	784.5
75	0.85	0.86	102.045	0.007×10^{16}	83020	813.2

Table 3: Measured Hall parameters of WSe_2 single crystal **sample 21**) in the temperature range 300K-20K for 4KG magnetic field

Temp. T(K)	Factor A	Factor B	Resistivity ρ(Ω.cm)	Carrier Density n(cm^{-3})	Hall coefficient R_H(cm^3/C)	Mobility μ (cm^2/Vs)
300	0.97	0.97	2.872	4.55×10^{16}	137.2	48.43
280	0.98	0.98	3.109	3.15×10^{17}	19.76	6.36
260	0.99	0.98	3.332	2.25×10^{18}	2.76	0.83
240	0.99	0.98	3.579	2.08×10^{17}	29.93	8.36
220	0.99	0.98	4.056	6.59×10^{17}	9.47	2.33
200	0.99	0.99	4.771	1.94×10^{17}	32.04	6.71
180	0.99	0.99	5.688	1.44×10^{17}	43.07	7.56
160	0.99	0.98	7.39	5.08×10^{16}	122.8	16.61
140	0.98	0.94	8.719	4.47×10^{16}	139.8	14.71
120	0.96	0.81	11.401	1.11×10^{17}	56.51	2.65
100	0.98	0.29	15.556	9.10×10^{15}	686.1	72.27
80	0.01	0.01	0.100	4.43×10^{14}	14080	60650
60	0.70	0.01	99.842	8.83×10^{14}	7070	63.41
40	0.94	0.95	7309	5.67×10^{13}	110200	31.25
20	0.93	0.01	8621	1.44×10^{11}	43270000	4719

Table 4: Measured Hall parameters of WSe_2 single crystals (**sample:22**) in the temperature range **300K-10K** for **4KG** magnetic field

Temp. T(K)	Factor A	Factor B	Resistivity ρ(Ω.cm)	Carrier Density n(cm^{-3})	Hall coefficient R_H(cm^3/C)	Mobility μ (cm^2/Vs)
300	0.98	0.98	2.797	1.032×10^{18}	6.049	2.141
290	0.98	0.97	2.918	6.554×10^{17}	9.524	3.266
270	0.98	0.98	3.077	2.924×10^{18}	2.135	0.695
250	0.99	0.98	3.309	5.443×10^{17}	11.47	3.464
230	0.99	0.98	3.639	1.297×10^{17}	48.12	13.22
210	0.99	0.99	4.259	8.187×10^{16}	76.25	17.91
190	0.99	0.99	5.101	5.410×10^{16}	115.4	22.65
170	0.99	0.99	6.557	9.967×10^{16}	62.63	9.632
150	0.99	0.98	8.913	2.226×10^{16}	280.5	31.46
130	0.99	0.97	13.02	9.088×10^{15}	686.9	50.85
110	0.99	0.83	18.447	9.215×10^{15}	677.4	2.852
90	1.00	0.35	19.734	1.147×10^{15}	5444	113.7
70	0.18	0.01	1.624	1.085×10^{15}	5754	185.7E+2
50	0.99	0.72	1461	9.81×10^{13}	63630	183.8
30	0.98	0.75	17541	5.324×10^{12}	1173E+3	67.58
10	0.01	0.01	5938	2.363×10^{11}	26420E+3	3205E+2

Thus it is evident that the few samples with Ag alloy wires gives a good ohmic behavior between the pairs of contacts and the average resistance between the contact pairs is found to be 1.5KΩ. The van der Pauw factor for geometry A and B for this sample is 0.99 and 0.99 respectively.

The low temperature experiments carried out for the three samples (samples 17, 21 and 22) have showed the deterioration of van der Pauw factor with temperature. At low temperatures below 100K the leakage current starts developing and the contact resistance increases substantially. But for good samples contact, the ohmic behaviour of the contact pairs remains the same and there is only a little change in van der Pauw factor. Figure 5 (a), (b) and (c) shows the dependence of the temperature on van der Pauw factor from 300K-75K, 300k-20K and 300K-10K respectively for samples 17, 21 and 22. The van der Pauw factor remains equal to 0.999 (nearly 1) for almost all measurement temperature up to 100K and slightly departs as temperature reaches to 10K in the sample 21 and 22. Whether sample 17 show lower range of van der pauw factor. That means ohmic nature of sample 17 is found to be poor.

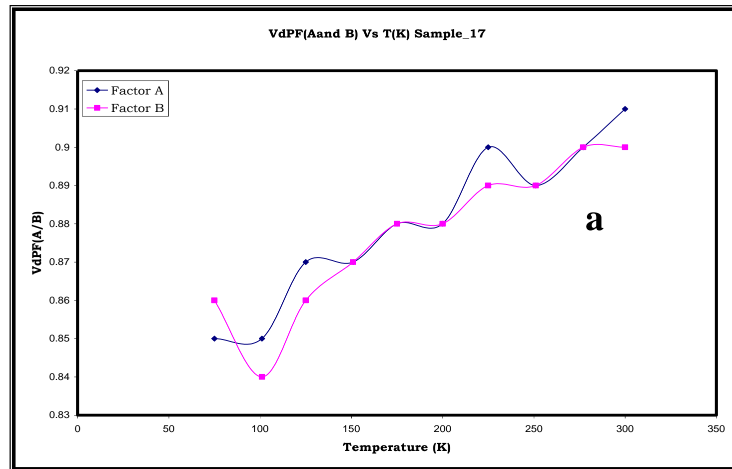

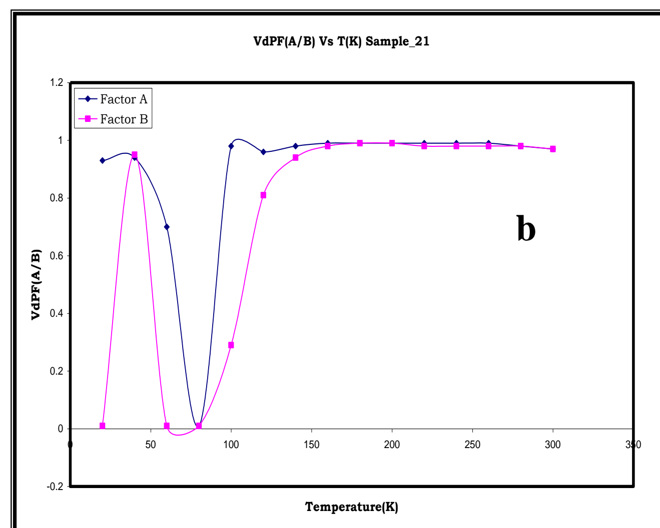

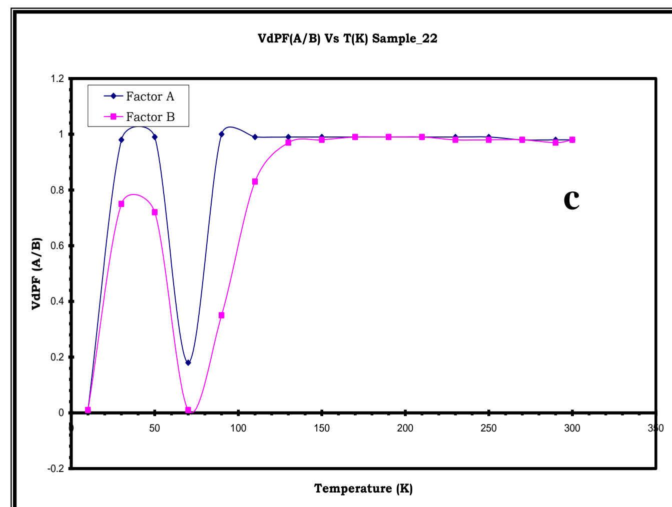

Figure 5:(a),(b) and (c) Stability curve of Van der Pauw factor with respect to temperature for samples 17,21 and 22 of WSe_2 crystals ranging from 300K-75K, 300K-20K and 300K-10K respectively.

Even though from the Hall effect measurements carried out on different samples as discussed above, a consistent set of observations have been chosen to evaluate temperature dependence of Hall resistivity, mobility, carrier concentration etc. of WSe_2 single crystals. The measured Hall parameters of such a typical set of observations are tabulated above.

The temperature dependence of hall parameters such as resistivity, carrier density and Hall mobility for sample 17, 21 and 22 is shown in figures 6 to 8.

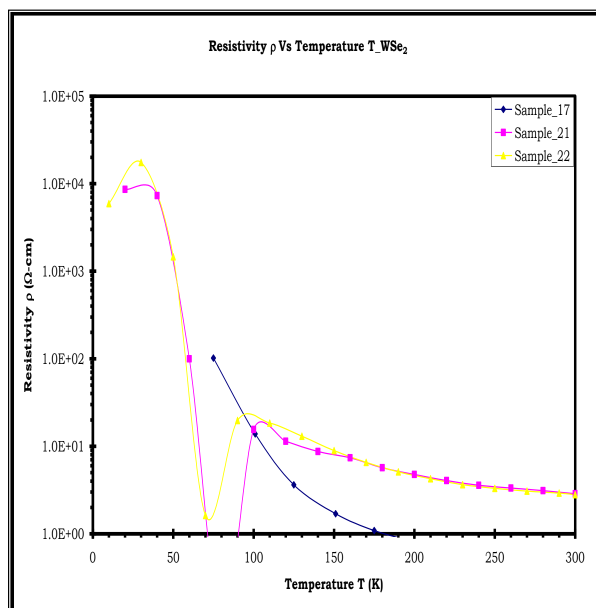

Figure 6: Temperature dependence of resistivity of WSe_2 single crystal for sample 17, 21 and 22 respectively.

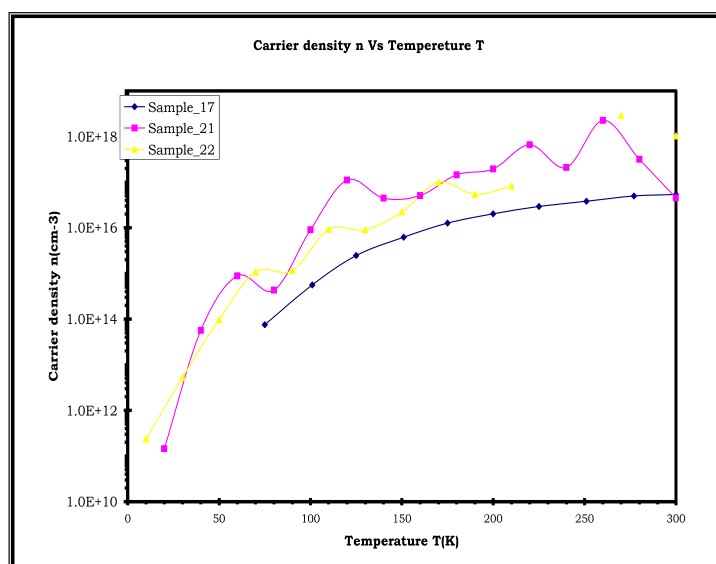

Figure 7: Temperature dependence of carrier density of WSe_2 single crystal for sample 17, 21 and 22 respectively

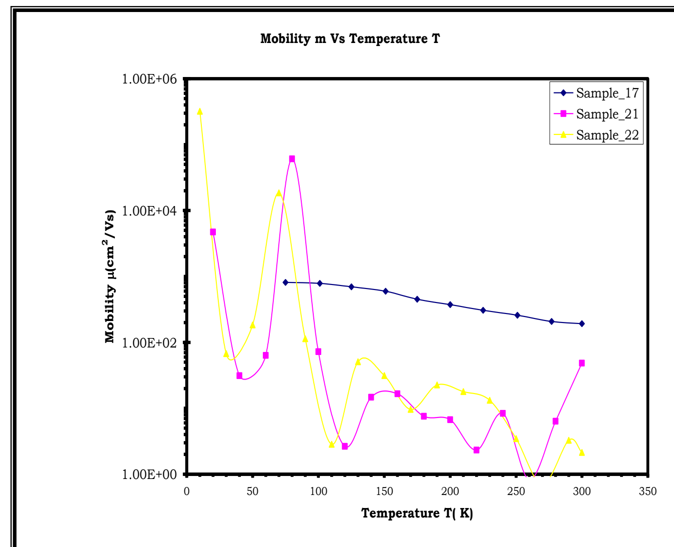

Figure 8: Temperature dependence of mobility of WSe_2 single crystal for sample 17, 21 and 22 respectively.

From the above plot, it has been conclude that increase in resistivity, decrease in carrier density and little increase in mobility found in all three samples of WSe_2 single crystal with low temperature range.

3.1 TEMPERATURE DEPENDENCE OF HALL COEFFICIENT

It can be seen that from the previous exercise in figure 4 and 5 three samples have been chosen as good ohmic contact. However sample 22 give consistent results for room temperature as well as low temperature hall measurements shown in Table 4. So the subsequent section is thus referred to the analysis of these measurements carried out for sample 22. The Hall coefficient R_H is directly related to the free carrier density n of the semiconductor by, R_H = r/ep or R_H = -r/en, where e is the electron charge and r is the Hall scattering factor, n and p are electron density and hole density respectively. Therefore from the measurement of the Hall coefficient the conductivity nature of the semiconducting material can be easily found. From the measurements of Hall voltage and current along with the magnetic field reversal the two Hall coefficients for both the geometries as discussed above were found (equations 13 and 14).The average Hall coefficient was then calculated using equation 15.

It is seen that it has an activated nature with positive temperature coefficient confirming that the crystals are of p-type semiconducting in nature.(see Table 4 and figure 9)

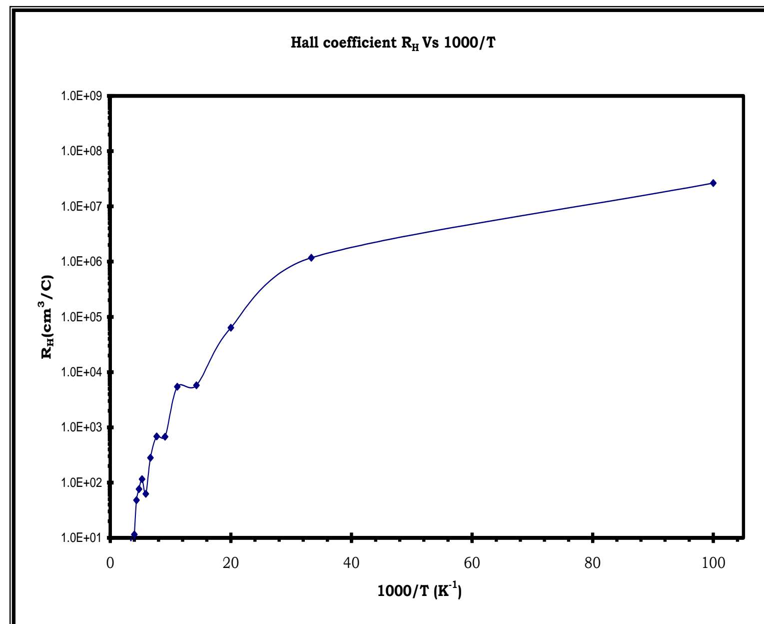

Figure 9: Hall coefficient versus reciprocal of temperature for WSe_2 single crystals, sample 22.

Three regimes are distinguished clearly from the figure. In the first region of temperature range (300K-70K) the value of R_H increases gradually. A transition occurs from 50K-10K temperature and the value of R_H increases by ten times and more in magnitude. This behaviour can be explained from the temperature dependent relationships of conductivity and carrier density and discussed below.

3.2 TEMPERATURE DEPENDENCE OF RESISTIVITY AND CARRIER DENSITY

The resistivities of as grown crystals sample evaluated from the equations 7 and 8, along the basal plane have been measured for a temperature range of 300K to 10K. In order to study the temperature dependence of the resistivity, the semi-log plot of the resistivity as a function of inverse temperature is presented in figure 10. It is clear from the tables 4 that as temperature decrease resistivity increases. Also from the graph it can be seen that the resistivities in the given temperature range show an activated nature. From this the temperature dependence of conductivity of WSe_2 crystals has been studied. The temperature variation of the conductivity of crystals plotted is shown in figure 11. Since WSe_2 crystals have been seen to have transition to intrinsic nature around 400-600K [13], the observed conductivity is in extrinsic region.

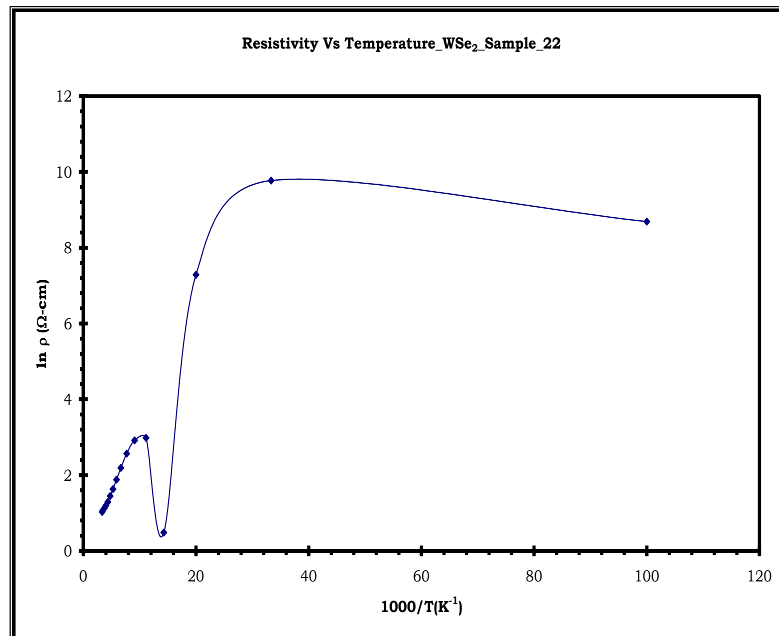

Figure 10: Semi-log resistivity as a function of inverse temperature for WSe_2 crystals, sample 22.

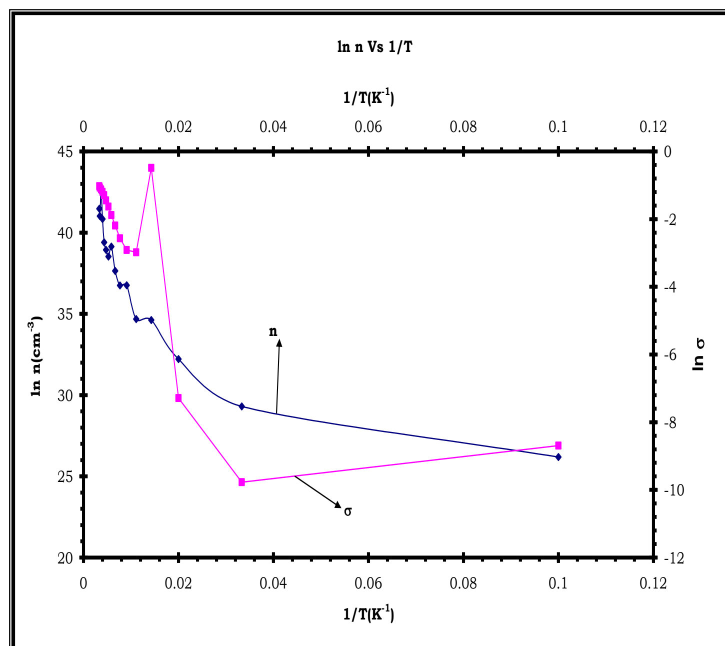

Figure 11: Temperature dependence of conductivity and carrier density of WSe_2 single crystal sample 22.

This is also confirmed by values of activation energies (table 6) as evaluated from figure 11 for the three identified temperature regions. The conductivity of a semiconducting material can have contributions from temperature dependence of carrier concentration and their mobility. The temperature dependence of carrier concentration as found is shown in figure 11.

Table 5: Variation of Fermi energy with temperature for sample 22 in the temperature range 300K-10K

T(K)	E_f (eV)
300	0.055
290	0.063
270	0.022
250	0.054
230	0.076
210	0.075
190	0.072
170	0.053
150	0.064
130	0.063
110	0.057
90	0.055
70	0.041
50	0.038
30	0.028
10	0.011

It shows similar temperature regions but having activation energies (table 6) different from that observed for the conductivity. The type of carriers as seen from the sign of Hall coefficient is p-type for 300K-10K. It is also seen that carrier concentration is decrease with low temperature.

Table 6: Activation energy for different temperature regions.

Temp. Range (K)	Carrier concentration (cm^{-3})	Activation energy (eV)	
		ln σ vs 1/T	ln n vs 1/T
300-70	10^{18}-10^{15}	0.040	0.050
50-30	10^{13}-10^{12}	0.038	0.064
30-10	10^{11}	1.6x10-5	1.38x10-6

WSe_2 is known to have layered structure with various polytypes having different stacking structures developing on conditions prevailing during preparation [15]. It has been found from XRD analysis that present crystals belongs to 2-H WSe_2 polytype similar to one reported in JCPDS –International Centre for Diffraction Data [16].

However, EDAX of our crystals show a slight selenium variation. The extrinsic electrical behavior of WSe_2 is generally attributed to the presence of both donors and acceptor impurities originating in defect structure of such crystals incorporated during its growth. Thus electrical behavior of crystals grown in the present study, which is predominantly p-type in most of the temperature range of investigation, can be attributed to the compensating nature of such defects. In present case it is very likely that selenium variation result in giving larger number of acceptor defects in comparison to shallower doner defects. This contention is also supported by the fact that selenium deficiency has been observed to give p-type [17] behavior with Fermi level moving towards valance band with decreasing selenium contents. Thus observed conductivity behavior of our crystals can be explained on a model of one acceptor and one shallower doner level in association with acceptor density N_A greater than donor defect density N_D. Accepter ionization energy is found to be 0.08eV and at high temperature region activation energy is almost half of this value. In compensated semiconductors, this originates due to change in the charge neutrality conditions for the two regions [18].

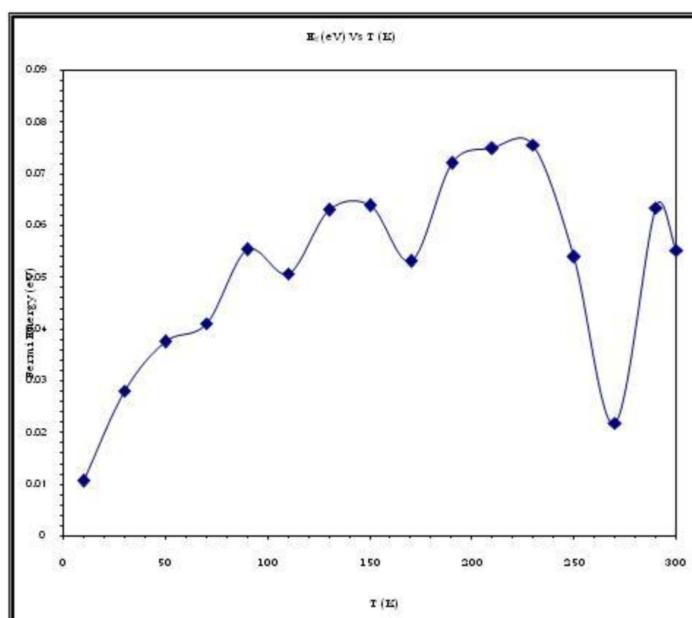

Figure 12: Temperature dependence of Fermi energy of WSe_2 in the temperature range 300K-10K for sample 22.

That is in higher temperature region carrier concentration $n>N_A$ while in lower temperature region $n<N_A$. This transition is also indicated from variation of Fermi level with temperature (figure 12). The Fermi energy [13] has been calculated from,

$$E_f = kT \ln\left(\frac{n}{N_c}\right) \tag{17}$$

Where N_c, the effective density of states for the conduction band and is given by,

$$N_c = 2\left(\frac{2\pi m^* k_B T}{h^2}\right)^{3/2} \tag{18}$$

It may be noted that in calculation of Fermi level the effective mass of carriers m^* has been used as $0.5m_e$ as founds from reports [19].

6.3.3 TEMPERATURE DEPENDENCE OF HALL MOBILITY

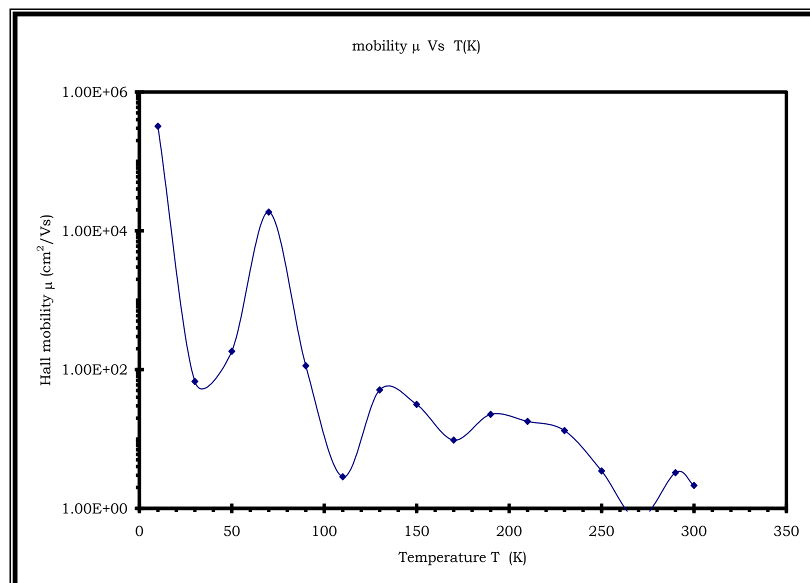

Figure 13: Variation of Hall mobility with temperature of WSe_2 for sample 22

Knowing the value of resistivity and Hall coefficient the Hall mobility Was calculated using the equation 16. The Hall mobility thus obtained in the temperature range of 300k-10K is tabuled in Table 4. The Hall mobilities derived from the experiment for different samples were found to be of the order of 1.82 to 6517cm^2/Vsec at room temperature, and they exhibit a temperature

dependence of the form $\mu \propto \left(\frac{T}{T_0}\right)^{-n}$. Since the WSe_2 semiconducting compounds possess a layered structure with covalent bonds within each layer and weak van der Waals forces between layers, and therefore this material shows highly anisotropic behaviour. This results in a short-range interaction between excess charge carriers and optical lattice vibrations, which is specific for layered structures. This was shown by Fivaz and Mooser [20], the structures like WSe_2, the free charge carriers tend to become localized within individual layers and thus to behave as if moving through a stack of independent layers. This tendency is accompanied by a strong interaction between the free carriers and the optical phonons polarized normally to the layers. The mechanism of this interaction can readily be visualized by describing the layers as independent potential wells whose widths vary with the elastic deformations of the lattice. Within the adiabatic approximation the width of a layer determines the energy of localization of a free carrier in this layer. Variation of the width, therefore, represents a perturbation which gives rise to a friction of the carrier. Width changing deformations occur in layers, like those of WSe_2 which are composed of several atomic planes, and they involve optical phonons polarized along normal to the layer. In an external electric field the charge carrier distribution may therefore be expected to relax predominantly through scattering by optical modes, if the temperature is high enough for these modes to be excited.

The mobility variation of WSe_2 with temperature (figure 13) shows again three temperature regions of mobility as mentioned it for the conductivity and carrier concentration. Therefore the temperature dependence of the carrier mobilities of WSe_2 has been evaluated by $\mu \propto \left(\frac{T}{T_0}\right)^{-n}$ to determine about the scattering mechanisms that limit the carrier mobilities. For temperature range 300K-100K the exponent n is found to be 1.1, which fit the experimental curve, with optical phonon energy ($\hbar\omega$)=0.005eV leads to acoustic-mode scattering. In layer structures only the horizontal dilations significantly modify the potential, the influence of the vertical ones being negligible because of the weakness of the Van der Waals forces between layers. Thus the carriers only interact with the horizontally polarized acoustic modes. By standard procedure it can be shown that the acoustic mode scattering leads to a charge carrier mobility which is inversely proportional to T [20]. As temperature lowers at 100K to 70K a sudden increase of mobility has been observed and this assigns the n value 2.46 and $\hbar\omega$ about 0.05eV. Again the temperature between 70K to 40K mobility has been decrease rapidly. The high value of n thus shows the strong temperature dependence of mobility and may be due to homopolar optical scattering mechanism. As the temperature decreases further below 40K the

value of mobility increases and here the value of n is found to be 1.5 with $\hbar\omega$, 0.2. This leads to a changeover of phonon scattering mechanism to ionized impurity scattering.

In the case of ionized impurity scattering, the lower temperature leads to a lower thermal velocity, with the electrons passing ionized impurity sites more slowly and suffering a stronger scattering effect. As a result the mobility μ_{ion} decreases with temperature.

Thus at a sufficiently high temperature the phonon scattering dominates, and the overall mobility will initially increase with decreasing temperature until the ionized impurity scattering becomes dominant.

The value of Hall coefficient and carrier density were use to find out Hall scattering factor from the relation,

$$R_H = \frac{r}{ep} \quad (19)$$

The value of Hall scattering factor is found to be 0.99 to 1 (table 6.7) for the temperature range 10K to 300K. From the value of 'r' the drift mobility is calculated by the relation,

$$\mu_H = |R_H \sigma| = r\mu . \quad (20)$$

The scattering process are characterized by mean relaxation time τ , which in turn related to the electron mobility μ_d according to (Smith, 1978) [21,22],

$$\mu_d = \frac{e\tau}{m^*} \quad (21)$$

Here for WSe_2 the calculated value of drift mobility and the relaxation time is tabulated in table 6.7. The angular frequency of the motion ω_c is calculated from the relation,

$$\omega_c = \frac{2\pi}{T} = \frac{eB_x}{m^*} . \quad (22)$$

For low field, $\omega_c \tau = \mu B_x << 1$ is satisfied and according to the energy dependant relaxation time theory the value of $\omega_c^2 \tau^2 << 1$ leads to the r value to be unity and is also matched with present result. Figure 14 shows the variation of Hall scattering factor with temperature.

Table 7: Various scattering parameters of WSe_2 sample 22

T(K)	Hall Scattering factor r	μ_d (cm^2/Vs)	τ(s)
300	0.999	2.14	6.01×10^{-16}
290	0.998	3.26	9.17×10^{-16}
270	0.997	0.69	1.95×10^{-16}
250	0.998	3.46	9.73×10^{-16}
230	1.000	13.20	3.72×10^{-15}
210	0.999	17.90	5.03×10^{-15}
190	0.999	22.60	6.36×10^{-15}
170	0.999	9.62	2.71×10^{-15}
150	1.000	31.50	8.86×10^{-15}
130	0.999	50.80	1.43×10^{-14}
110	0.999	2.85	8.02×10^{-16}
90	1.000	114.00	3.20×10^{-14}
70	1.000	1.86×10^{4}	5.2×10^{-12}
50	0.999	184.00	5.16×10^{-14}
30	0.998	67.50	1.90×10^{-14}
10	0.998	3.20×10^{5}	8.99×10^{-11}

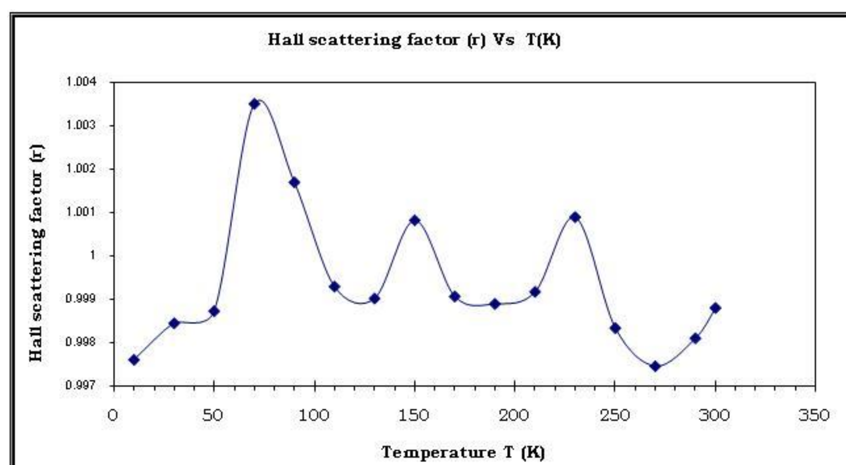

Figure 14: Variation of Hall scattering factor with temperature for WSe_2 single crystals for sample 22

CONCLUSION

WSe_2 crystals grown by DVT technique under conditions given are seen to possess semiconducting nature, which can be explained in terms of one donor and one shallower acceptor defect levels originating from growth conditions. The temperature dependence Hall coefficient study revealed that the grown crystal shows mixed conduction behavior in the temperature region 300K to 10K. The variation of mobility with temperature, also show that the WSe_2 possesses a mixed scattering mechanism.

From room temperature to low temperature till 100K, it has been found that the acoustic mode scattering mechanism dominates. Strong temperature dependence on mobility could be observed thereafter from 100K–70K, where homopolar optical scattering mechanism may dominate and further decrease of the mobility with decreasing temperature may be attributed to the ionized impurity scattering. Thus measurements of Hall effect parameters carried out on a series of semiconducting tungsten dichalcogenides layer structures have shown that in these materials the charge carriers have the temperature dependent mobilities. The temperature dependence of the drift mobility has been derived from the experimental information and is tabulated in table 6.7.

The Hall scattering factor calculated from the temperature dependent Hall coefficient and carrier density, found to be 0.99 to 1. Due to the experimental limitation of low magnetic field, the effect of magnetic field on these could not be studied. Detailed analysis of temperature dependent Hall effect data thus yields information concerning the electronic transport properties of tungsten diselenide semiconducting layered materials.

REFERENCES

1. M. Zoaeter, A. Conan, D. Delaunay, Phys. Stat. sol. (a) **41** (1977) 629
2. L.J.Van der Pauw, Philips Res. Rep. **13** (1958)1
3. L J Van der Pauw, Philips Technical Review, **26** (1958) 220
4. W. Daniel Koon, Rev. Sci. Instrum. **69** (1998)
5. W. Daniel Koon, Rev. Sci. Instrum. **61 (9)** (1990)
6. W. Daniel Koon, Arshad A, Rev. Sci. Instrum. **64 (2)** (1993)
7. W. Daniel Koon, Rev.Sci. Instrum. **60 (2)** (1989)
8. Lake Shore 7500/9500 Series Hall System User's Manual
9. K. Dieter Schroder, (Ed.) (1990) Semiconductor Material and Device Characterization,John Wiley & sons, Inc. Publications
10. V. M. Pathak, Ph.D. thesis, Sardar Patel University, Vallabh Vidyanagar **43** (1990)
11. B. L. Evans, Hazelwood R A, Phys. stat. sol. (a) **4** (1971) 181
12. Huang Ying-Sheg, Chinees J. Phys. **22** (1984) 43
13. A. J. Grant, T. M. Griffiths, A. D. Yoffee, G. D. Pitt, J. Phys. C **8** (1975) L17.
14. R. Bourezg, G. Couturier, Salardenne J, Phys. Rev. B **46** (1992) 15 404
15. R. Pratap, D. L. Bhattacharya , Phys. stat. sol. (a) 12 61 (1972)
16. JCPDS, International Centre for Diffraction Data, (1997)
17. M. Zoaeter, A. Conan, Delaunay D, Phys. stat. sol. (a) 41 629 (1977)
18. J .S. Blakemore, J. Appl. Phys. 511054 (1980)
19. M. P. Deshpande, Ph.D.thesis (Sardar Patel University: India) p180 (1998)
20. R. Fivaz, E. Mooser, Phys. Rev. **163** (1967) 743
21. R. A. Smith, Semiconductors, Cambridge university press, (1978)
22. Blood P, Orton J W, The Electrical Characterization of Semiconductors: Majority Carriers and Electron States,Academic Press, **97** (1992)